IOP Conf. Series: Materials Science and Engineering **174** (2017) 012006 doi:10.1088/1757-899X/174/1/012006

Dynamic analysis of six-bar mechanical press for deep drawing

S Mitsi, I Tsiafis and K D Bouzakis

Laboratory for Machine Tools and Manufacturing Engineering, Mechanical Engineering Department, Aristotle University, University Campus, 54124 Thessaloniki, Greece

E-mail: mitsi@eng.auth.gr

Abstract. This paper analyzes the dynamical behavior of a six-bar linkage used in mechanical presses for metal forming such as deep drawing. In the under study mechanism, a four-bar linkage is connected to a slider through an articulated binary link. The motion of the six-bar linkage is studied by kinematic analysis developing an analytical method. Furthermore, using an iterative method and d' Alembert's principle, the joint forces and drive moment are evaluated considering joint frictions. The simulation results obtained with a MATLAB program are validated by comparing the theoretical values of the input moment with the ones obtained from the conservation of energy law.

1. Introduction

The mechanical press is widely employed for metal-forming processes. Many different types of linkage drives have been proposed to satisfy the load – stroke characteristics for the specific metal-forming process. The metal forming operations like shearing requires very short stroke of the ram and deep drawing requires a slow and long stroke of the punch. Yan and Chen [1, 2] proposed the novel approach of varying the input speed such that the ram's motion was suitable for both deep-drawing and precision-cutting processes. Hsieh and Tsai [3] developed a novel press system with six links for precision deep drawing so that can generate complicated and flexible output motion. Soong [4] proposed a new design method for single DOF mechanical press with variable speeds and length-adjustable driving links. Yossifon and Shivpuri [5] investigated the design, analysis and construction of a double knuckle press for precision forming driven by a servo motor. The dynamic analysis of the double-toggle press, performed in [6], included the evaluation of bearing forces and the required input torque without considering joint friction. Tso and Liang [7] proposed a nine-bar linkage for mechanical presses in order to obtain slow forming speed and a long period of dwell time in the bottom of the ram stroke. The dynamic analysis and simulation of a hybrid-driven two-degrees-of-freedom seven-bar press using Lagrangian's formulation have been developed by Li and Zhang [8]. The force analysis of a six-linkage used in mechanical presses for metal forming such as coining and blanking, considering joint frictions is presented in [9].

In the present paper the dynamic analysis of a six-bar linkage for mechanical press used for the deep drawing, is investigated. First, the kinematic analysis, dealing with the displacement, velocity and acceleration of the mechanism links, is performed. Then, the force analysis, taking into account the external force and joint frictions, is presented.

2. Kinematic analysis of six-bar linkage

The investigated mechanical press contains a six-bar linkage (figure 1). An electrical motor provides the input torque to the crank through a gears transmission. The six-bar linkage is composed of the A_0ABB_0 four-bar linkage connected to the slider through the articulated binary link CD. Structural, this mechanism includes the frame 0, the input link 1 and the second-class Assur group RRR (links 2 and 3) connected to the second-class Assur group RRP (links 4 and 5) through the revolute joint C, where R denotes a revolute pair and P a prismatic pair. The joints A_0 and B_0 are fixed and the input link 1 rotates with a constant known angular velocity ω_{10}. Also the link lengths $l_0=A_0B_0$, $l_1=A_0A$, $l_2=AB$, $l_{AC}=AC$, $l_3=B_0B$, $l_4=CD$ and the distance a are given.

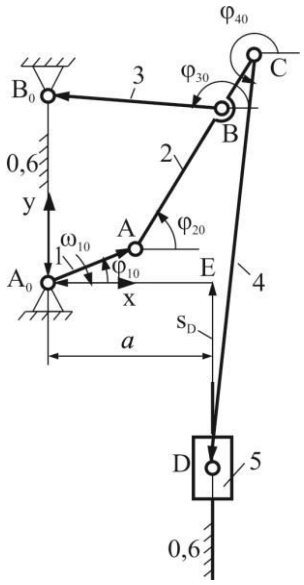

Figure 1. Kinematic model of six-bar mechanical press.

The equations for kinematic analysis are written and solved considering a Cartesian coordinate system, with origin the joint A_0. The mechanism has two independent closed contours $A_0ABB_0A_0$ and A_0ACDEA_0. Every link length and slider displacement (from a convenient reference point E) are represented by suitable planar vectors. The vector equation corresponding to each above independent closed loop is:

For closed contour $A_0ABB_0A_0$:

$$\boldsymbol{l_1} + \boldsymbol{l_2} + \boldsymbol{l_3} + \boldsymbol{l_0} = \boldsymbol{0} \tag{1}$$

and for closed contour A_0ACDEA_0:

$$\boldsymbol{l_1} + \boldsymbol{l_2} + \boldsymbol{l_4} + \boldsymbol{s_D} + \boldsymbol{a} = \boldsymbol{0} \tag{2}$$

The vector equations (1) and (2) are projected on the Cartesian reference system. It is obtained:

$$l_1 cos\varphi_{10} + l_2 cos\varphi_{20} + l_3 cos\varphi_{30} = 0 \tag{3}$$

$$l_1 sin\varphi_{10} + l_2 sin\varphi_{20} + l_3 sin\varphi_{30} - l_0 = 0 \tag{4}$$

$$l_1 cos\varphi_{10} + l_{AC} cos\varphi_{20} + l_4 cos\varphi_{40} - a = 0 \tag{5}$$

$$l_1 sin\varphi_{10} + l_{AC} sin\varphi_{20} + l_4 sin\varphi_{40} + s_D = 0 \tag{6}$$

Equations (3) and (4) constitute a set of two nonlinear equations in two unknowns, namely φ_{20} and φ_{30}. To determine the angle φ_{20}, the equations (3) and (4) are rearranged as:

$$l_3 cos\varphi_{30} = -l_1 cos\varphi_{10} - l_2 cos\varphi_{20} \tag{7}$$

$$l_3 sin\varphi_{30} = -l_1 sin\varphi_{10} - l_2 sin\varphi_{20} + l_0 \quad (8)$$

Squaring the equations (7) and (8) and adding them, the following equation is obtained:

$$A\, cos\varphi_{20} + B\, sin\varphi_{20} = C \quad (9)$$

where:

$$A = -2 l_1 l_2 cos\varphi_{10}$$

$$B = 2\left(l_0 - l_1 sin\varphi_{10}\right) l_2$$

$$C = l_2^2 - l_3^2 + l_1^2 cos^2\varphi_{10} + \left(l_0 - l_1 sin\varphi_{10}\right)^2 \quad (10)$$

Equation (9) has the solutions [9]:

$$\varphi_{20} = atan\left(C/\left(\pm\left(A^2 + B^2 - C^2\right)^{1/2}\right)\right) - atan\left(A/B\right) \quad (11)$$

The double sign "±" in equation (11) corresponds to the two different assembly modes of RRR Assur group.

The angle φ_{30} is obtained using a similar procedure eliminating the angle φ_{20} from equations (3) and (4).

For each value of the angle φ_{20}, using equation (5), the angle φ_{40} is determined [9]**:**

$$\varphi_{40} = atan\left(\pm\left(1 - D^2\right)^{1/2} / D\right) \quad (12)$$

with $D = \left(a - l_1 cos\varphi_{10} - l_{AC} cos\varphi_{20}\right) / l_4$. The double sign "±" in equation (12) corresponds to the two different assembly modes of RRP Assur group.

Finally, once φ_{20} and φ_{40} are known, from equation (6) the slider displacement s_D is obtained:

$$s_D = -l_1 sin\varphi_{10} - l_{AC} sin\varphi_{20} - l_4 sin\varphi_{40} \quad (13)$$

It has been mentioned that from the four configurations of the six-bar linkage, the one that corresponds to the working specifications of the mechanical press is chosen.

The results of displacement analysis are used for velocity analysis. Differentiating equations (3) and (4) with respect to time and after rearranging terms it is obtained a set of two linear equations in the unknown angular velocities ω_{20} and ω_{30}. By solving this system the unknown velocities are determined as [9]:

$$\omega_{20} = \left(\omega_{10} l_1 sin\left(\varphi_{10} - \varphi_{30}\right)\right) / \left(l_2 sin\left(\varphi_{30} - \varphi_{20}\right)\right) \quad (14)$$

$$\omega_{30} = \left(\omega_{10} l_1 sin\left(\varphi_{20} - \varphi_{10}\right)\right) / \left(l_3 sin\left(\varphi_{30} - \varphi_{20}\right)\right) \quad (15)$$

where $\omega_{i0} = d\varphi_{i0} / dt \ \ (i = 1, 2, 3)$.

Differentiating equation (5) with respect to time, a linear equation in unknown angular velocity ω_{40} is obtained and the solution is:

$$\omega_{40} = \left(-l_1 \omega_{10} sin\varphi_{10} - l_{AC} \omega_{20} sin\varphi_{20}\right) / \left(l_4 sin\varphi_{40}\right) \quad (16)$$

The slider velocity v_D is determined by solving the linear equation obtained by differentiating equation (6) with respect to time:

$$v_D = -l_1 \omega_{10} cos\varphi_{10} - l_{AC} \omega_{20} cos\varphi_{20} - l_4 \omega_{40} cos\varphi_{40} \quad (17)$$

Acceleration analysis is performed by differentiating the equations derived in velocity analysis with respect to time. From the obtained equations are determined the angular accelerations ε_{20}, ε_{30}, ε_{40} and the slider acceleration a_D:

$$\varepsilon_{20} = \left(A_1 cos\varphi_{30} + B_1 sin\varphi_{30}\right) / \left(l_2 sin\left(\varphi_{30} - \varphi_{20}\right)\right) \quad (18)$$

$$\varepsilon_{30} = -\left(A_1 cos\varphi_{20} + B_1 sin\varphi_{20}\right) / \left(l_3 sin\left(\varphi_{30} - \varphi_{20}\right)\right) \quad (19)$$

$$\varepsilon_{40} = \left(a_{xC} - l_4 \omega_{40}^2 cos\varphi_{40}\right) / \left(l_4 sin\varphi_{40}\right) \quad (20)$$

$$a_D = -a_{yC} - l_4\varepsilon_{40}cos\varphi_{40} + l_4\omega_{40}^2 sin\varphi_{40} \quad (21)$$

where:

$$A_1 = l_1\omega_{10}^2 cos\varphi_{10} + l_2\omega_{20}^2 cos\varphi_{20} + l_3\omega_{30}^2 cos\varphi_{30}$$
$$B_1 = l_1\omega_{10}^2 sin\varphi_{10} + l_2\omega_{20}^2 sin\varphi_{20} + l_3\omega_{30}^2 sin\varphi_{30}$$
$$a_{xC} = -l_1\omega_{10}^2 cos\varphi_{10} - l_{AC}\varepsilon_{20}sin\varphi_{20} - l_{AC}\omega_{20}^2 cos\varphi_{20}$$
$$a_{yC} = -l_1\omega_{10}^2 sin\varphi_{10} + l_{AC}\varepsilon_{20}cos\varphi_{20} - l_{AC}\omega_{20}^2 sin\varphi_{20}$$

The results of kinematic analysis are furthermore used to calculate the accelerations of the link mass centers needed to perform the kinetostatic analysis of the mechanism.

3. Forces analysis

The kinetostatic force analysis takes into account the inertia forces and moments imposed on the links and the joint friction forces considering known the ram force F_{ext}. The ram external force is opposed to the motion of the link 5. The friction losses are due to the sliding friction at the contact area between the ram 5 and the frame and the friction moment in revolute joints. In the calculation of friction forces and moments, the joint reaction forces, the characteristic property of the joint materials in contact and the relative velocities are considered.

The determination of the joint reaction forces and the input moment is performed using an iterative procedure [9]. After kinematic analysis, the joint reaction forces and the input moment are calculated without friction. At the solution step m+1 of the iterative procedure, friction forces and moments are assumed to be external loads that have been defined during the determination of the joint reaction forces at the previous iteration step m. The iterative procedure converges when the difference between two successive values of the obtained joint reaction forces is smaller than a prescribed criterion ε that indicates the desired accuracy of the calculation. The solution converges rapidly due to the low values of the friction forces and moments.

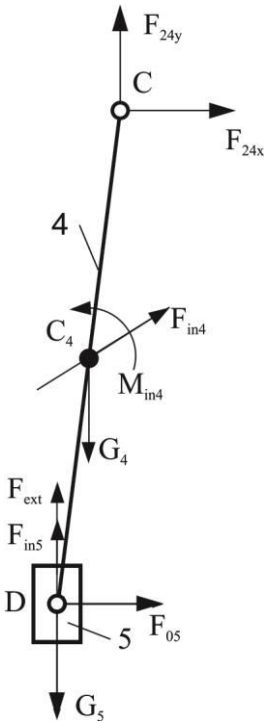

Figure 2. RRP (4, 5) dyad forces.

Due to decupled structure of the mechanism, the equations for the force analysis are written and solved separately for each Assur group (dyad) and input link 1 considering D' Alembert principle. In each link k, the inertia force F_{ink} (k=1,n, n=links number) is assumed to act at the mass center C_k and an inertia moment M_{ink} is added.

The dynamic analysis starts with the RRP (4, 5) dyad because the external force $\mathbf{F_{ext}}$ is known. Figure 2 shows the forces and the moments that act on the RRP (4, 5) dyad. The unknown joint reaction forces are $\mathbf{F}_{45}$= - $\mathbf{F}_{54,}$ $\mathbf{F}_{05}$ and $\mathbf{F}_{24}$. The joint reaction $\mathbf{F}_{05}$ is perpendicular to the sliding direction of the ram 5. To calculate the reactions forces, a force equation for links 4 and 5 and a moment equation on link 4 are written.

The vector sum of all the forces that act on the links 4 and 5 is zero:

$$\boldsymbol{(4,\ 5)} - \boldsymbol{\Sigma F} = \boldsymbol{F_{24} + G_4 + G_5 + F_{in4} + F_{in5} + F_{ext} + F_{05} = 0} \quad (22)$$

and the vector sum of all the moments on link 4 about D is zero:

$$\boldsymbol{4} - \boldsymbol{\Sigma M_D} = \boldsymbol{r_{DC} \times F_{24} + r_{DC4} \times (G_4 + F_{in4}) + M_{in4} = 0} \quad (23)$$

where G_4 and G_5 are gravitational forces of links 4 and 5 respectively. The vectorial equations (22) and (23) give three scalar equations on x, y and z, that form a linear system of three equations with three scalar unknowns F_{24x}, F_{24y} and F_{05x}. For solving this system of equations the MATLAB program is used. The joint reaction force $\mathbf{F_{45}}$ is calculated from the force equation for link 5:

$$\boldsymbol{5} - \boldsymbol{\Sigma F} = \boldsymbol{F_{45} + F_{in5} + G_5 + F_{ext} + F_{05} = 0} \quad (24)$$

The application point of the reaction force $\mathbf{F_{05}}$, calculated from a moment equation about D for link 5, is at D.

Figure 3 shows the forces and the moments that act on the RRR (2, 3) dyad. The unknown joint reaction forces are $\mathbf{F}_{03}$, $\mathbf{F}_{32}$ and $\mathbf{F}_{12}$. The joint force $\mathbf{F_{42}} = -\mathbf{F_{24}}$ was calculated from the previous RRP (4, 5) dyad.

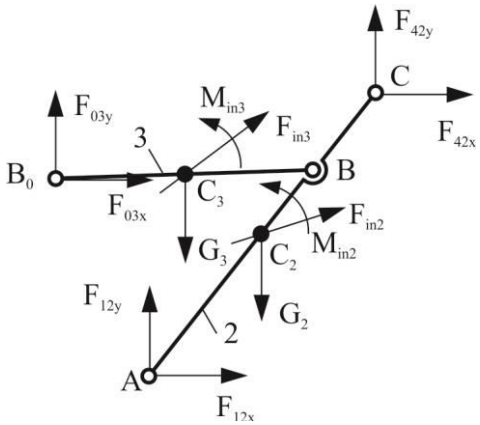

Figure 3. D' Alembert principle for RRR (2, 3) dyad.

The vector sum of all the forces that act on links 2 and 3 is zero:

$$(2,\ 3)\ -\Sigma F = F_{12} + F_{42} + G_2 + G_3 + F_{in2} + F_{in3} + F_{03} = 0 \tag{25}$$

The vector sum of all the moments on link 2 about B is zero:

$$2 - \Sigma M_B = r_{BA} \times F_{12} + r_{BC2} \times (G_2 + F_{in2}) + r_{BC} \times F_{42} + M_{in2} = 0 \tag{26}$$

and the vector sum of all the moments on link 3 about B is zero:

$$3 - \Sigma M_B = r_{BB0} \times F_{03} + r_{BC3} \times (G_3 + F_{in3}) + M_{in3} = 0 \tag{27}$$

The vectorial equation (25) gives two scalar equations on x and y and equations (26) and (27) give one scalar equation on z, that form a linear system of four equations with four scalar unknowns F_{03x}, F_{03y}, F_{12x} and F_{12y}. For solving this system of equations the MATLAB program is used.

The joint reaction force $\mathbf{F_{32}}$ is calculated from the force equation for link 2:

$$2 - \Sigma F = F_{12} + F_{in2} + G_2 + F_{42} + F_{32} = 0 \tag{28}$$

The force analysis without friction ends with the input link 1. Figure 4 shows the forces and moments that act on the input link. The unknowns are the joint reaction force $\mathbf{F}_{01}$ and the input moment (motor moment) $\mathbf{M_{mot}}$. The joint force $\mathbf{F_{21}} = -\mathbf{F_{12}}$ was calculated from the previous dyad RRR.

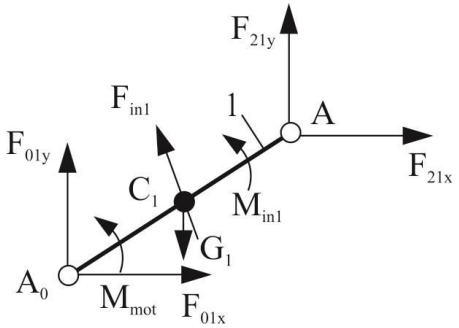

Figure 4. D' Alembert principle for input link 1.

The joint reaction force $\mathbf{F_{01}}$ is calculated from the force equation for link 1:

$$\boldsymbol{1-\Sigma F = F_{01} + F_{in1} + G_1 + F_{21} = 0} \tag{29}$$

and the input moment $\mathbf{M_{mot}}$ is determined from the equation of moments with respect A_0:

$$\boldsymbol{1-\Sigma M_{A0} = M_{mot} + r_{A0A} \times F_{21} + r_{A0C1} \times (G_1 + F_{in1}) + M_{in1} = 0} \tag{30}$$

The joint reaction forces without friction are used furthermore in the first step of the iterative procedure to analyze the forces considering the joint frictions. At the solution step m+1 of the iterative procedure, friction forces and moments are calculated with the aid of reaction forces F_{ij}^{m} determined at the step m.

The friction moment M_{fij}^{m+1} at the revolute joint ij, opposed to relative angular velocity ω_{ji}, is:

$$M_{fij}^{m+1} = -sign\,(\omega_{ji})\,\mu\, r_{ij} F_{ij}^{m} \qquad (i,\ j = 0, \ldots, 5) \tag{31}$$

and the friction force F_{f05}^{m+1} at the prismatic joint D is:

$$F_{f05}^{m+1} = -sign\,(v_{50})\,\mu\, F_{05}^{m} \tag{32}$$

where μ is friction coefficient and r_{ij} is joint shaft radius.

These friction moments and friction force, considered to be external loads, are introduced in the corresponding equations of the method above described to calculate the joint reaction forces and input moment at step m+1.

4. Numerical application

The above equations have been implemented in a computer program using MATLAB software to generate the simulation presented throughout the paper. The main dimensions of the six-bar linkage (figure 1) used for kinematic analysis are inserted in table 1. These dimensions have been chosen in order to assure an approximately constant and small velocity and, accordingly, a quick return suitable for deep drawing. The driver link 1 rotates with a constant angular velocity of ω_{10}=-4 rad/s. All five moving links are rectangular prism with depths d_1=5 mm, d_2=d_3=8 mm, d_4=10 mm, d_5=20 mm and heights h_1=2 mm, h_2=h_3=4 mm and h_4=5 mm, h_5=16 mm. The density of the material is ρ_{steel}= 8000 kg/m^3. The joint shaft radii are: r_{A0}=r_D= 20 mm, r_A=r_B= r_{B0}= r_C= 30 mm and the friction coefficient is μ=0.1. The center of mass of links 1 and 5 is located in the joint A_0 and joint D respectively.

Table 1. Main dimensions of six-bar press.

Dimensions	l_0	l_1	l_2	l_3	l_{AC}	l_4	l_5	a
(mm)	128	64	112	112	160	290	80	110

The ram external force is opposed to the motion of the link 5: F_{ext} = - sign(v_D)F_e, where F_e=10^6 N throughout the working stroke.

The results for the kinematic simulation are shown in figures 5 and 6. Figure 5 shows the ram displacement (a), velocity (b) and acceleration (c) of the forming mechanical press. It is observed, that in the working zone, the ram velocity is approximately constant and has small values (figure 5b). The links positions for a complete rotation of the driver link 1 (the step of the angle is 10^0) are given in figure 6.

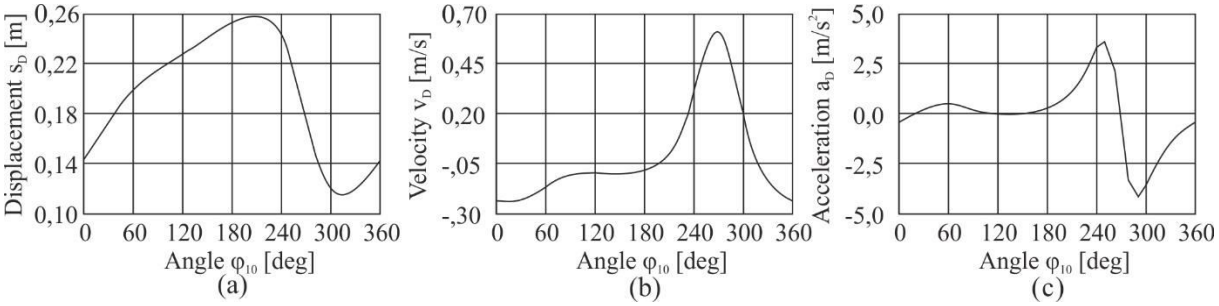

Figure 5. Displacement (a), velocity (b) and acceleration (c) of ram.

Some results for the dynamic simulation are shown in figures 7 and 8. Figure 7 illustrates the x, y components of the joint reaction forces F_{01} (a) and F_{03} (b) respectively versus crank angle with and without friction. In figure 8a is given the input torque versus crank angle with and without friction.

In order to validate the simulation results obtained with the MATLAB program, the values of the input torque without friction (method 1 in figure 8b) are compared with the ones obtained from the conservation of energy law (method 2 in figure 8b). It is remarked a very good agreement of the results.

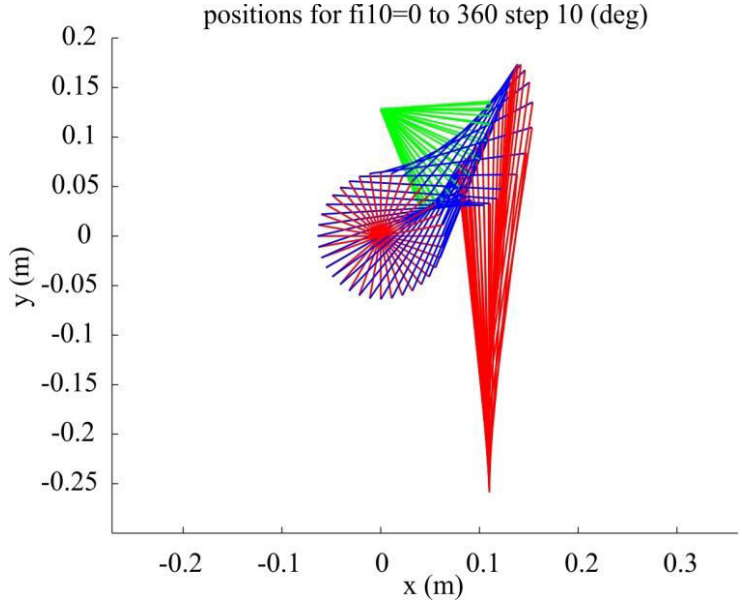

Figure 6. The link positions of six-bar press along the entire ram stroke.

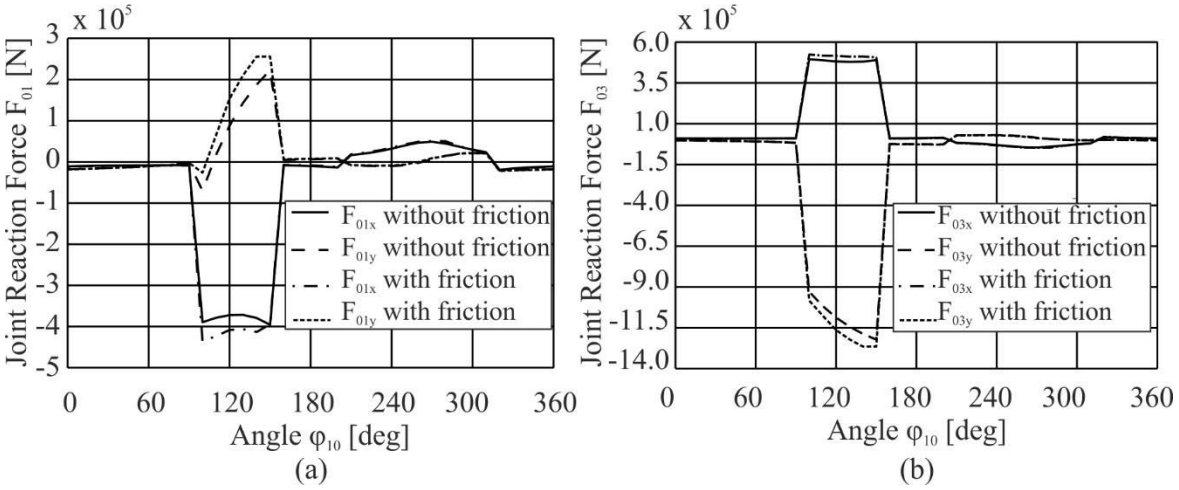

Figure 7. Joint reaction forces F_{01} (a) and F_{03} (b).

5. Conclusions

In the current study, the kinematic and kinetostatic analysis of a six-bar linkage of a mechanical press for deep drawing has been investigated developing a MATLAB program. An analytical method has been used for the determination of the displacement, velocity and acceleration of the links and the simulation of mechanism motion. The force analysis considering the joint friction is performed with

an iterative procedure, applying the D'Alembert principle. It is observed that due to the low values of the friction forces and moments, the solution converges after one iteration step. The developed program can be useful for the optimization of the press design considering different constraints.

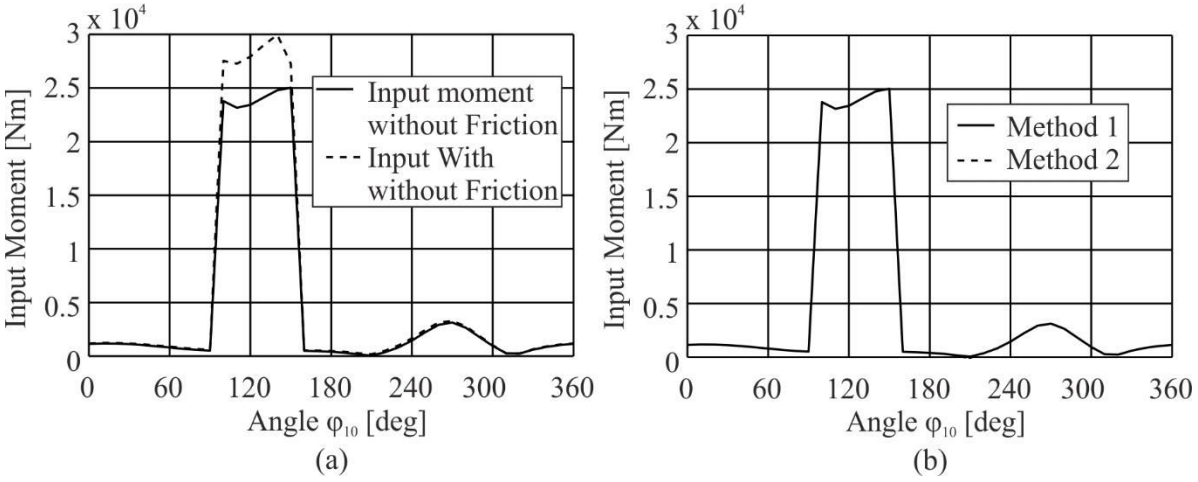

Figure 8. Input moment versus crank angle.

References

[1] Yan H S and Chen W R 2000 A variable input speed approach for improving the output motion characteristics of Watt-type presses *Int J Mach Tools Manuf* **40** 675
[2] Yan H S and Chen W R 2002 Optimized kinematics properties for Stevenson-type presses with variable input speed approach *Trans ASME J Mech Des* **124** 350
[3] Hsieh W H and Tsai C H 2011 On a novel press system with six links for precision deep drawing *Mech Mach Theory* **46** 239
[4] Soong R Ch 2010 A new design for single DOF mechanical presses with variable speeds and length-adjustable driving links *Mech Mach Theory* **45** 496
[5] Yossifon S and Shivpuri R 1993 Analysis and comparison of selected rotary linkage drives for mechanical presses *Int J Mach Tools Manuf* **33** 175
[6] Yossifon S and Shivpuri R 1993 Design considerations for the electric servo-motor driven 30 ton double kniehle press for precision forming *Int J Mach Tools Manuf* **33** 209
[7] Tso P L and Liang K C 2002 A nine-bar linkage for mechanical forming presses *Int J Mach Tools Manuf* **42** 139
[8] Li H and Zhang Y 2010 Seven-bar mechanical press with hybrid-driven mechanism for deep drawing Part 2 Dynamic modelling and simulation *J Mech Sci Technol* **24** 2161
[9] Mitsi S, Tsiafis I and Bouzakis K D 2015 Force analysis of six-bar linkage for mechanical presses considering joint frictions *J Balk. Tribol. Assoc.* **21** 281